

curve in Fig. 2(b) illustrates the result of such a calculation for  $N = 2 \times 10^{18} \text{ cm}^{-3}$  in CdS. Since the EHL has a rather small compressibility for compression to densities larger than  $N_0$  the excitation is expected to expand into the crystal until this density is achieved as indicated by the data shown in Fig. 2(a). However, at higher temperatures expansion beyond  $N_0$  to the equilibrium density at the sample temperature is not observed. There is evidence that in Si at higher temperatures expansion of an initially overdense plasma ( $N \approx N_0$  but greater than the equilibrium density) takes a time on the order of  $10\text{--}20 \times 10^{-9} \text{ sec}$ .<sup>11</sup> This time is considerably longer than the excitation lifetime in a direct-gap material like CdS so it is unlikely that the equilibrium density can be achieved by expansion beyond  $N_0$  during the excitation lifetime. These considerations suggest that the droplets of liquid expected to form for the case of underdense pumping can be expected to have rather small radius.

In conclusion we have investigated condensation of optically excited carriers in the direct-gap semiconductor CdS and find that the liquid phase can form from an underdense gas of excitation up to temperatures  $\approx 55^\circ\text{K}$ . These results determine the liquid portion of the gas-liquid coexistence curve for this system. While our understanding of condensation phenomena in the limit of pulsed, high-intensity excitation is not complete, we find that our results are in good agreement with similar measurements made under quite different pumping conditions for Ge, and indirect-gap material with very different excitation decay kinetics. The short lifetime of the excitation, and the high density of the liquid phase in CdS might be expected to create very different conditions governing the condensation process; nevertheless,

our results demonstrate that the factors determining the liquid portion of the coexistence curve for EHL's are quite general with similar behavior for materials having very different band structures.

<sup>1</sup>R. F. Leheny and Jagdeep Shah, *Phys. Rev. Lett.* **37**, 871 (1976).

<sup>2</sup>V. G. Lysenko, V. I. Revenko, T. G. Tratas, and V. B. Timofeev, *Zh. Eksp. Teor. Fiz.* **68**, 335 (1975) [*Sov. Phys. JETP* **41**, 163 (1975)].

<sup>3</sup>G. O. Müller, in *Proceedings of the Taormina Research Conference on the Structure of Matter: Recent Developments in Optical Spectroscopy of Solids*, Taormina, Italy, 1976 (to be published), and private communication.

<sup>4</sup>G. Beni and T. M. Rice, *Phys. Rev. Lett.* **37**, 874 (1976).

<sup>5</sup>T. L. Reinecke and S. C. Ying, *Phys. Rev. Lett.* **35**, 311 (1975).

<sup>6</sup>K. L. Shaklee, R. E. Nahory, and R. F. Leheny, *J. Lumin.* **7**, 284 (1974).

<sup>7</sup>All temperatures reported are sample temperatures. For the pump intensity used carrier heating is not expected to be significant. [See J. Shah, *Phys. Rev. B* **9**, 562 (1974).]

<sup>8</sup>While this assumption gives a good fit to the data as in the case GaAs [E. Göbél, *Appl. Phys. Lett.* **24**, 492 (1975)] further investigation of the EHL line shape in direct-gap materials is required.

<sup>9</sup>The details of this calculation will be published in a longer article describing this work, but the calculation is essentially the same as the graphical construction used by M. Combescot [*Phys. Rev. Lett.* **32**, 15 (1974)] to determine  $T_c$  for Ge.

<sup>10</sup>G. A. Thomas, T. M. Rice, and J. C. Hensel, *Phys. Rev. Lett.* **33**, 219 (1974).

<sup>11</sup>Jagdeep Shah and A. H. Dayem, *Phys. Rev. Lett.* **37**, 861 (1976).

## Computer Model of Metallic Spin-Glasses

L. R. Walker and R. E. Walstedt  
*Bell Laboratories, Murray Hill, New Jersey 07974*  
 (Received 6 January 1977)

The properties of dilute Ruderman-Kittel-Kasuya-Yosida-coupled classical spins randomly embedded in an fcc lattice have been investigated by computer simulation. Results at  $T = 0$  are given for spatial correlations, molecular-field distributions, susceptibility, and frequencies of elementary excitations. Treating the latter as bosons, we find quantitative agreement with measured specific-heat values. The susceptibility  $\chi(0)$  is also in accord with experiment.

A characteristic property of experimental spin-glass systems is that the low-temperature specific heat is approximately linear in  $T$  and substan-

tially independent of concentration  $c$  over some considerable range of  $c$ .<sup>1,2</sup> Attempts to explain this behavior on the basis of single spin excita-

tions<sup>3-5</sup> require that there be a finite probability of essentially vanishing molecular field acting on a spin. Convincing arguments that this can occur with the isotropic Ruderman-Kittel-Kasuya-Yosida (RKKY) coupling which prevails in these systems have not been given.<sup>6</sup>

In the Letter we report the results of a computer simulation of a realistic spin-glass intended to clarify the low-temperature behavior of such a system. The model consists of dilute, randomly distributed classical spins on an fcc lattice; the coupling is of the isotropic RKKY form. We determine equilibrium configurations relevant to  $T=0$  and study their elementary excitations. The spectrum of excitations is found to extend continuously from zero up to the interaction energy of nearest-neighbor pairs. Low-lying modes are extended, involving all the spins in the sample. As the excitation energy rises, many of the modes acquire local character and the highest (pair) modes are completely localized. The distribution and density of mode energies are such as to give a quantitative account of the specific heat  $C_m(T)$  for values of  $T$  well below the spin-glass ordering temperature  $T_c$ . We also present results on the molecular-field distributions as well as the short-range correlation distance and the zero-temperature susceptibility. The results given provide the first quantitative understanding of low-temperature properties of spin-glass systems.

Systems of  $N=96$  and 324 spins, distributed randomly in a cubic section of fcc lattice, were studied at average concentrations  $c$  of 0.3% and 0.9%. The interaction between spins  $\vec{n}_i$  and  $\vec{n}_j$  was taken to have the asymptotic RKKY form

$$\begin{aligned} E_{ij} &= -A\vec{n}_i \cdot \vec{n}_j \cos(2k_F r_{ij} + \varphi) / r_{ij}^3 \\ &= -J_{ij} \vec{n}_i \cdot \vec{n}_j. \end{aligned} \quad (1)$$

The finite system of  $N$  spins was extended throughout all space through the use of periodic boundary conditions. Accordingly, the range of the interaction was truncated<sup>7</sup> at  $r_{ij}=d/2$ , where  $d$  is the dimension of the cubic cell, to prevent double interactions. The Fermi wave vector  $k_F$  was taken to be that for Cu metal, and  $\varphi$  was arbitrarily set to zero. The main results are expected to be essentially independent of  $\varphi$ .

The total energy of the system is minimized when each vector,  $\vec{n}_i$ , points along the exchange field  $\vec{h}_i = \sum_j J_{ij} \vec{n}_j$ . Such configurations were reached by sequentially rotating each  $\vec{n}_i$  to lie along the current  $\vec{h}_i$  and iterating this process.

Since the dependence of the energy on  $\vec{n}_i$  has the form  $-\vec{n}_i \cdot \vec{h}_i$ , the above procedure must decrease the total energy at every step. Convergence to alignment can be accelerated by repeatedly extrapolating all the spin trajectories forward after a cycle of iterations.

During equilibration, which starts from random initial orientations, the spins come very quickly into a "quasiequilibrium" state wherein each spin is aligned with its molecular field to within  $\sim 1^\circ$ . There follows a rather slow second phase, during which the energy decreases very slowly and almost exclusively by means of an increase in the average magnitude of the exchange fields. The remarkable feature of this second phase is that the spins continue to move through rather large angles toward their equilibrium positions. For example, in one typical case of 96 spins, the spins moved through an average angle of  $\sim 16^\circ$  while the energy changed by 0.1% and the mean deviation  $\langle \theta_i \rangle = \langle \cos^{-1}(\vec{n}_i \cdot \vec{h}_i / |\vec{h}_i|) \rangle$  went from  $0.23^\circ$  to  $0.06^\circ$ . This behavior is indicative of a very low exchange stiffness for an equilibrium configuration (EC). When rotation and inversion degeneracies are eliminated, EC's generated from random starting orientations seem to consist of different arrangements of nearly identical subregions containing  $\sim 20$  spins. Our data are insufficient to predict the variation of the number of energy minima with  $N$ .

In a dilute system of randomly oriented spins it is easily shown that the distribution of exchange-field moduli  $P(h)$  is given by<sup>8</sup>

$$P(h) = (4\Delta h / \pi) h^2 / (h^2 + \Delta h^2)^2. \quad (2)$$

In Eq. (2),  $\Delta h = \frac{1}{3}\pi^2 c A n_0 \langle |\cos(2k_F r_{ij} + \varphi)| \rangle_{av}$ , where  $n_0$  is the density of sites. In the present case, one has  $\Delta h = 8\pi c A / 3a^3$ , where  $a$  is the fcc lattice constant. Apart from minor deviations resulting from the finite concentration of our system, Eq. (2) is borne out to within statistical accuracy by computer-generated random distributions. For an EC the deviation from Eq. (2) is surprisingly small, as shown in Fig. 1. There the closed circles show a plot of Eq. (2) adjusted to have the same area as the molecular-field histogram. The primary effect of ordering is thus seen to be a broadening of  $P(h)$  by  $\sim 20\%$ . A second, more subtle effect is the disappearance of spins having very low exchange fields. (No spin was ever found in the lowest interval of the histogram.) This is the opposite of the effect suggested in Ref. 5 and can be accounted for in terms of short-range correlations. A study of the latter has re-

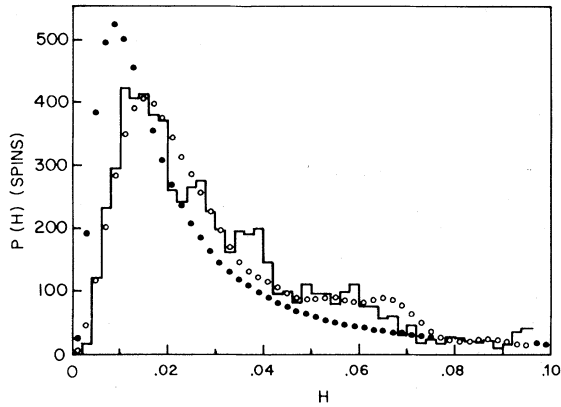


FIG. 1. Histogram of ordered-state exchange-field moduli in reduced units for 324 spins at  $c=0.3\%$ . Filled circles, Eq. (2) plotted with area adjusted to equal that of the histogram. Open circles, model calculation described in text.

vealed that the correlation volume, defined by the condition  $0.5 \leq \langle \vec{n}_i \cdot \vec{n}_j \rangle_{av} \leq 1.0$ , encloses an average of  $\sim 1.7$  neighbors of a given spin. The average contribution to  $\vec{h}_i$  from correlated components of the exchange field may be written  $|\vec{h}_i|_{corr} \cong \sum_j J_{ij} \langle \vec{n}_i \cdot \vec{n}_j \rangle_{av}$ , where the summand is  $\geq 0$ , and  $\langle \vec{n}_i \cdot \vec{n}_j \rangle_{av} \rightarrow 0$  as  $r_{ij} \rightarrow \infty$ . This expression shows that there are no cancellation effects between contributions to  $|\vec{h}_i|_{corr}$ , thus explaining the general increase of molecular fields on ordering exhibited in Fig. 1. Furthermore, the only way to achieve a very small field is to have *no* spins in any of a number of strongly coupled neighbor shells, which is an event of low statistical probability. The effect of random components of spin can be incorporated by convolving a histogram of the  $|\vec{h}_i|_{corr}$ 's with a suitably calculated broadening function. With this simple picture we have calculated the model distribution in Fig. 1 shown by the open circles. The gross features of the ordered distribution are seen to be correctly represented in this way, including the hole in the distribution at  $h=0$ .

Classically, the frequencies of small oscillations about a given EC are found by linearizing the equation of motion,  $d\vec{n}_i/dt = \vec{n}_i \times \vec{h}_i$ , with  $\vec{n}_i = \vec{n}_{i0} + \delta\vec{n}_i(t)$  (where  $|\delta\vec{n}_i| \ll 1$ ). Defining a Cartesian coordinate system ( $\vec{a}_i, \vec{b}_i, \vec{n}_i^0$ ) at each site, one finds  $2N$  linear equations for the amplitudes of the  $\vec{a}_i$  and  $\vec{b}_i$  components of the  $\delta\vec{n}_i$ . The associated matrix, whose eigenvalues are  $\pm i\omega$ , has the form  $\begin{vmatrix} 0 & -1 \\ 1 & 0 \end{vmatrix} \mathcal{E}$ , where  $\mathcal{E} = \begin{vmatrix} A & B \\ B^* & C \end{vmatrix}$  is the matrix of the quadratic form expressing the energy for small displacements. The  $N \times N$  submatrices are given by  $A_{ij} = \lambda_i \delta_{ij} - J_{ij} \vec{a}_i \cdot \vec{a}_j (1 - \delta_{ij})$ ;  $B_{ij} = -J_{ij} \vec{a}_i$

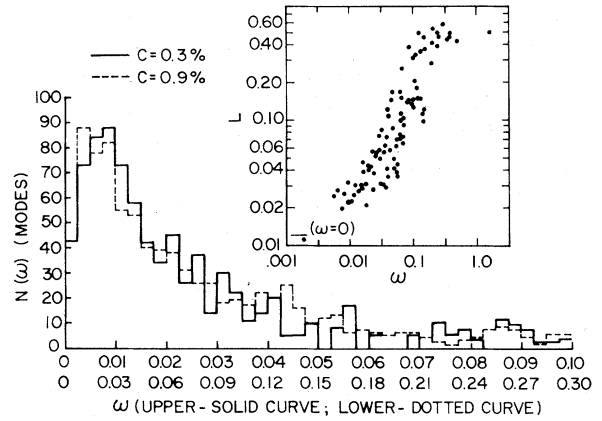


FIG. 2. Histograms of elementary excitation frequencies in reduced units for  $c=0.3$  and  $0.9\%$  calculated with  $N=96$  spin arrays. Inset, log plot of localization indices (see text) vs frequency for a particular spatial distribution.

$\vec{b}_i (1 - \delta_{ij})$ ; and  $C_{ij} = \lambda_i \delta_{ij} - J_{ij} \vec{b}_i \cdot \vec{b}_j (1 - \delta_{ij})$ . In a quantum mechanical treatment one takes the spins to lie initially along  $\vec{n}_i^0$  and writes the transverse displacements in terms of boson annihilation and creation operators. By retention of quadratic terms, these may be diagonalized by a Bogoliubov transformation. The frequencies are the same as the classical ones and the parameters of the transformation are connected simply to the classical  $\vec{a}_i$  and  $\vec{b}_i$  amplitudes. The classical calculation then contains all numerical information needed for the quantum problem.

The excitation frequencies were calculated using EC's of 96 spins. Mode-density histograms compiled from 10 different spatial distributions each for  $c=0.3\%$  and  $c=0.9\%$  are shown in Fig. 2 in the same units as in Fig. 1. The excitation spectrum is seen to have a markedly different shape from the field distribution, with a high density of modes at frequencies well below the peak of  $P(h)$ . A number of high-frequency satellite modes are off the scale of Fig. 2. The continuum region shown is seen to scale with concentration as expected. Some light is thrown on the nature of the excitation modes by examining the localization indices  $L_\mu = \sum_i W_{i\mu}^2 / (\sum_i W_{i\mu})^2$ , where  $W_{i\mu} = |\alpha_{i\mu}|^2 + |\beta_{i\mu}|^2$  is the weight coefficient for spin  $i$  in mode  $\mu$ , and  $\alpha_{i\mu}$  and  $\beta_{i\mu}$  are defined by

$$\delta\vec{n}_{i\mu}(t) = (\alpha_{i\mu} \vec{a}_i + \beta_{i\mu} \vec{b}_i) \exp(i\omega_\mu t) + c.c. \quad (3)$$

Values of  $L_\mu$  are  $\sim 1$  and  $N^{-1}$  for localized and extended modes, respectively. A plot of  $L_\mu$  vs  $\omega_\mu$

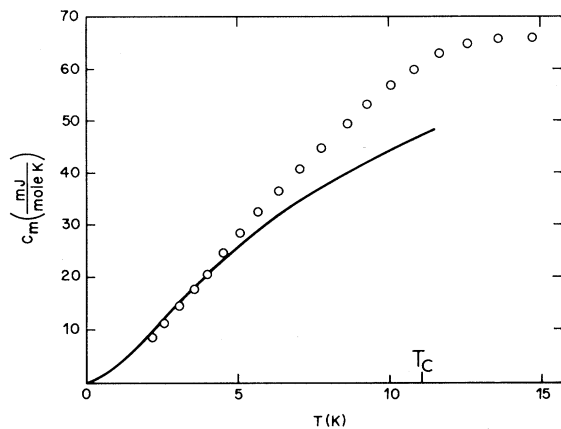


FIG. 3. Solid curve, molar specific heat from model calculated as described in text. Circles, data for 1.2% Mn in Cu from Wenger and Keesom (Ref. 2).

for 96 mode pairs is shown as an inset to Fig. 2. There is an essentially continuous distribution of  $L_\mu$ 's down to the extended limit,  $N^{-1}=0.01$ . It appears that almost all modes with  $\omega > 0.05$  are substantially localized and those with  $\omega < 0.05$  are extended. There are four zero-frequency modes (three of which correspond to uniform rotations). Such modes are an  $N^{-1}$  effect and are omitted from the histogram of Fig. 2.

The magnetic-specific-heat contribution is given by the temperature derivative of  $E(T) \cong E_g + \sum_\mu \langle n_\mu \rangle \hbar \omega_\mu$ , where  $\langle n_\mu \rangle = [\exp(\hbar \omega_\mu / kT) - 1]^{-1}$ . A molar specific heat curve calculated with this equation using the  $c=0.9\%$  mode-density histogram of Fig. 2 (scaled to  $c=1.2\%$ ) is shown in Fig. 3 in comparison with experimental data on  $\text{Cu}_{0.988}\text{Mn}_{0.012}$  given by Wenger and Keesom.<sup>2</sup> The temperature scale of the calculated curve corresponds to an RKKY coefficient  $A = 9.5 \times 10^{-37}$  erg  $\text{cm}^3$ , slightly smaller than the value  $A = (12.0 \pm 1.4) \times 10^{-37}$  erg  $\text{cm}^3$  given by Smith.<sup>9</sup> On close inspection, the extrapolated experimental data curve in Fig. 3 is seen to intersect the  $T$  axis at  $T \sim 1$  K. This strongly suggests the presence of a gap in the frequency spectrum at  $\omega = 0$ . Although a small gap is found in the frequency spectra of Fig. 2, it would not materially affect the calculated curve for  $C_m$ . The latter curve does not exhibit as pronounced a frequency-gap characteristic as do the data. We conclude that some gap-producing feature is not present in our model—possibly a source of anisotropy in the Hamiltonian. The range of agreement in Fig. 3 extends to  $T \sim T_c/3$ , as might be expected for a spin-wave calculation.

EC's have also been used to calculate the zero-

temperature susceptibility  $\chi(0)$ . The calculation is a classical one, yielding (in reduced units)

$$\chi(0) = \sum_{\lambda'} \left\{ \sum_i (\xi_{i\lambda} \hat{a}_i \cdot \hat{a} + \eta_{i\lambda} \hat{b}_i \cdot \hat{a}) \right\}^2 / E_\lambda, \quad (4)$$

where  $(\xi_{1\lambda}, \dots, \xi_{N\lambda}, \eta_{1\lambda}, \dots, \eta_{N\lambda})$  is an eigenvector of the energy matrix  $\mathcal{E}$  defined earlier and  $E_\lambda$  is the corresponding eigenvalue. The prime on  $\sum_\lambda$  in Eq. (4) denotes omission of the three  $\lambda$ 's for which  $E_\lambda = 0$  from the sum. The spurious contribution from these rotation modes is nullified by taking the unit vector  $\hat{a}$  in the direction of the net moment  $\sum_i \vec{n}_i$ . With the same value of  $A$  used in Fig. 3, we find  $\chi(0) = 1.7 \times 10^{-3}$  emu/mole  $\pm 15\%$  at  $c=0.9\%$ . This is in good agreement with experimental values  $\chi(0) = 1.5 \times 10^{-3}$  emu/mole for 1.3% Mn in Cu<sup>10</sup> and  $\chi(0) = 2.0 \times 10^{-3}$  emu/mole for 0.97% Mn in Cu.<sup>11</sup>

In conclusion, we find that an approach in which spin-glass systems are viewed as conventional antiferromagnets with  $N$  sublattices leads to quantitative descriptions of the susceptibility and specific heat. The internal consistency of this picture is further supported by a calculated value of  $\sim 6\%$  for the zero-point reduction of the local magnetization, suggesting a relatively stable ground configuration. Further details of these calculations will be published elsewhere.

<sup>1</sup>J. Zimmerman and F. E. Hoare, Phys. Chem. Solids **17**, 52 (1960).

<sup>2</sup>L. E. Wenger and P. H. Keesom, Phys. Rev. B **13**, 4053 (1976).

<sup>3</sup>W. Marshall, Phys. Rev. **118**, 1520 (1960).

<sup>4</sup>M. W. Klein and R. Brout, Phys. Rev. **132**, 2412 (1963).

<sup>5</sup>N. Rivier, Phys. Rev. Lett. **37**, 232 (1976), and references therein.

<sup>6</sup>In the treatment given in Ref. 5, the Ising behavior seems to follow automatically from the doubtful assumption that the spins lie in certain fixed directions in space which are not determined, in turn, by the resulting fields. Another counter argument is given by P. W. Anderson, in *Amorphous Magnetism*, edited by H. O. Hooper and A. M. deGraaf (Plenum, New York, 1973), p. 1.

<sup>7</sup>This amounts to a neglect of random fields smaller than the histogram interval in Fig. 1.

<sup>8</sup>The analogous formula for the case of  $S = \frac{1}{2}$  was given by N. Rivier and K. Adkins, in *Amorphous Magnetism*, edited by H. O. Hooper and A. M. deGraaf (Plenum, New York, 1973), p. 215. The calculation is easily extended to the present case.

<sup>9</sup>F. W. Smith, Phys. Rev. B **14**, 241 (1976). In Smith's notation,  $A = V_0 S$ . We prefer to take  $S = \frac{5}{2}$  and attribute the diminished saturation moment to  $g < 2$ , leading to a slightly smaller value for  $A$  than is given by Smith's analysis.

<sup>10</sup>V. Cannella, in *Amorphous Magnetism*, edited by

H. O. Hooper and A. M. deGraaf (Plenum, New York, 1973), p. 195.

<sup>11</sup>J. A. Careaga, B. Dreyfus, R. Tournier, and L. Weil, in *Proceedings of the Tenth International Con-*

*ference on Low Temperature Physics, Moscow, U. S. S. R., 1966*, edited by A. S. Borovik-Romanov and V. A. Tulin (VINITI Publishing House, Moscow, 1967), Vol. IV, p. 284.

## Lossless and Dissipative Current-Carrying States in Quasi-One-Dimensional Superconductors

L. Kramer

*IBM Zurich Research Laboratory, 8803 Rüschlikon, Switzerland, and Physik Department der Technischen Universität München, 8046 Garching bei München, West Germany\**

and

A. Baratoff

*IBM Zurich Research Laboratory, 8803 Rüschlikon, Switzerland*  
(Received 15 November 1976)

We present a global stability analysis of possible states in narrow current-carrying superconductors below  $T_c$  within time-dependent Ginzburg-Landau theory. A reversible superconducting-to-normal transition may take place at a current density  $j_c$  lower than the maximum supercurrent  $j_{\max}$ . Localized phase slip occurs spontaneously in a narrow range below  $j_c$ .

Current-induced transitions in superconducting filaments continue to be a puzzle. Simple "one-dimensional" situations where the coherence length  $\xi(T)$  and the penetration depth  $\lambda(T)$  are large compared to the transverse dimensions of the sample can be realized experimentally in the vicinity of the transition temperature  $T_c$ . Except very close to  $T_c$ , where fluctuation effects dominate, the normal state is approached through successive voltage jumps. The intervening states have been thoroughly investigated by Meyer<sup>1</sup> and Skocpol, Beasley, and Tinkham.<sup>2</sup> These authors relate them to the appearance of localized "phase-slip centers." Hysteresis appears a few millidegrees kelvin below  $T_c$ .

No satisfactory theory of these phenomena is available. The simplest time-dependent Ginzburg-Landau (TDGL) theory<sup>3,4</sup> is unable to explain the observed temperature-independent differential resistance presumably introduced by each center,<sup>2</sup> unless inhomogeneities much larger than  $\xi(T)$  are significant. Nevertheless, it can provide valuable insight into the situation. We present here a complete picture of possible states in an infinite homogeneous one-dimensional superconductor within that framework. Previous attempts in that direction<sup>5-7</sup> suffered from *ad hoc* assumptions. Recently, Likharev<sup>8</sup> found a special solution describing a superconducting-normal (SN) boundary moving with constant velocity. The latter vanishes at a well-defined current density  $j_c$  below the maximum supercurrent  $i_{\max}$ .

We show that the superconducting (alternatively the normal) state is in fact *globally unstable* above (below)  $j_c$ . Within a limited range  $j_{\min} < j < j_c$  we also find a new dissipative state describing *localized phase-slip* oscillations *spontaneously* occurring in a *homogeneous* filament. Boundary effects and results for weak links, which extend those of Likharev and Jakobson,<sup>9</sup> will be reported elsewhere.<sup>10</sup>

Our work is based on numerical and limiting analytic solutions of the one-dimensional TDGL equations,

$$u(\dot{\psi} + i\mu\psi) = \psi'' + (1 - |\psi|^2)\psi, \quad (1)$$

$$j = \text{Im}\psi^*\psi' - \mu'. \quad (2)$$

As in Ref. 9, the complex order parameter  $\psi$  is normalized so that its magnitude equals 1 for zero current; distance  $x$ , current density  $j$ , electrochemical potential  $\mu$ , and time  $t$  are measured in units of  $\xi(T)$ ,  $j_0 = (\hbar c/2e)c/4\pi\lambda^2\xi$ ,  $\mu_0 = ej_0\xi/\sigma_N$ , and  $t_0 = 4\pi\lambda^2\sigma_N/c^2 = \hbar/2\mu_0$ , respectively ( $\sigma_N$  is the conductivity in the normal state and  $t_0$  is the current relaxation time). Finally,  $u$  is the order-parameter relaxation time divided by  $t_0$ . Equations (1) and (2) can be rigorously derived in the so-called strong depairing limit for a dirty gapless superconductor; one then has  $u = 12$ . For weak depairing  $u = 5.79$ ,<sup>3</sup> but microscopic theory predicts important additional terms<sup>11,12</sup> which are not included here. We simply consider  $u$  as a parameter. The filament is assumed connected to a